

# Astrophysics of extreme mass ratio inspiral sources

Clovis Hopman

*Faculty of Physics, Weizmann Institute of Science, POB 26, Rehovot 76100, Israel; Leiden Observatory, P.O. Box 9513, NL-2300 RA Leiden. E-mail: clovis@strw.leidenuniv.nl*

**Abstract.** Compact remnants on orbits with peri-apses close to the Schwarzschild radius of a massive black hole (MBH) lose orbital energy by emitting gravitational waves (GWs) and spiral in. Scattering with other stars allows successful inspiral of such extreme mass ratio inspiral sources (EMRIs) only within small distances,  $a < \text{few} \times 0.01 \text{ pc}$  from the MBH. The event rate of EMRIs is therefore dominated by the stellar dynamics and content in the inner  $\text{few} \times 0.01 \text{ pc}$ . I discuss the relevant dynamical aspects and resulting estimated event rates of EMRIs. Subjects considered include the loss-cone treatment of inspiral sources; mass segregation; resonant relaxation; and alternative routes to EMRI formation such as tidal binary disruptions, stellar formation in disks and tidal capture of massive main sequence stars. The EMRI event rate is estimated to be of order  $\text{few} \times 10^2 \text{ Gyr}^{-1}$  per MBH, giving excellent prospects for observation by *LISA*.

**Keywords:** black hole physics — stellar dynamics — gravitational waves — Galaxy: center

**PACS:** 95.55.Ym, 95.85.Sz, 97.80.Kq, 98.10.+z, 97.60.Lf, 98.62.Js

## INTRODUCTION

One of the most exciting and plausible targets of the *Laser Interferometer Space Antenna* (*LISA*) is the inspiral of a stellar mass compact remnant (CR), i.e., a white dwarf (WD), neutron star (NS) or stellar black hole (BH), into a massive black hole (MBH) of mass  $M_{\bullet} \sim 10^6 M_{\odot}$ , or an intermediate mass black hole (IMBH) of  $M_{\bullet} \sim (10^3 - 10^4) M_{\odot}$ . Because of the large difference between the mass of the MBH and the CR, such sources are known as “extreme mass ratio inspirals” (EMRIs). *LISA* can detect stars with orbital periods  $1 \text{ s} < P < 10^4 \text{ s}$  at distances of  $\sim 1 \text{ Gpc}$ .

MBHs are embedded in dense stellar cusps, as was predicted theoretically [5, 6], and confirmed observationally in our own Galactic center [1, 16, 2]. Due to the high stellar density, the relaxation time, i.e., the time it takes a star to change its energy by order unity, is typically shorter than the age of the Universe. This implies that the orbits of stars can change due to dynamical encounters in the course of time: a star that is initially not on an orbit at which it loses much energy to gravitational waves (GWs), can be scattered to an orbit where energy losses to GWs are large, so that the star spirals in.

The short relaxation time of galactic nuclei complicates the analysis of EMRI rates, as is reflected by wildly differing estimates in the literature [20, 41, 33, 11, 26, 12, 3, 15, 21, 22, 23]. Here I discuss a framework in which EMRI dynamics can be analyzed. The most important result is that the EMRI rate is mostly determined by the dynamics and stellar content of the inner few  $0.01 \text{ pc}$ . Within this distance from the MBH, dynamical effects such as mass segregation and resonant relaxation are discussed. I also review some alternative EMRI formation scenarios, which differ from the direct capture model.

# LOSS-CONE DYNAMICS OF EMRIS

## Stars near a MBH: energy space

The distribution function (DF) of Newtonian point masses near a MBH was first found by Bahcall & Wolf [5] for a single mass population, and later generalized to a multi-mass population [6]. The Bahcall & Wolf solution is characterized by a density profile of stars that diverges towards the center. For a single mass population, the density is given by

$$n_{\star} \propto r^{-\alpha}, \quad (1)$$

with  $\alpha = 7/4$ . For a multi-mass population, the slope  $\alpha$  depends on mass. First, I focus on the single mass case, which captures much of the relevant physics. I later return to the important (but not much studied) case of a multi-mass population.

An interesting feature of the Bahcall & Wolf solution is that it is not only a steady state solution of the Fokker-Planck equation, but that in addition the flow of stars in energy space is very strongly suppressed compared to what one would expect from dimensional arguments. As a result of this, stars typically come close to the MBH due to scattering in their angular momenta rather than in their energies.

## Stars near a MBH: angular momentum space

Stars typically reach the MBH on wide orbits of low energy that are very eccentric (have very small angular momentum) [31, 6]. If there is some periapse  $r_p$  such that stars with periapse  $r_p < r_q$  are swallowed by the MBH, then this defines for loosely bound orbits a region in angular momentum space called the “loss-cone”, given by  $J_{lc} = \sqrt{2GM_{\bullet}r_q}$ . For CRs, the loss-cone is determined by the angular momentum of the last stable orbit in general relativity, which for an eccentric orbit is given by  $J_{lc} = J_{LSO} \equiv 4GM_{\bullet}/c$ .

Far away from the MBH, the changes  $\Delta J_p$  in angular momentum per orbit are much larger than the size of the loss-cone. This implies that a star for which  $J < J_{lc}$  at apo-apse may have  $J > J_{lc}$  at peri-apse and survive, and vice-versa: a star with  $J > J_{lc}$  at apo-apse may have  $J < J_{lc}$  at peri-apse and be swallowed. As a result, far away from the MBH, the DF can be isotropic, and for given semi-major axis the fraction of stars with angular momentum  $< J$  is given by  $(J/J_c)^2$ , where  $J_c$  is the angular momentum of a circular orbit. The rate at which stars are swallowed by the MBH in this “full loss-cone” regime is estimated by  $\Gamma(a)da \sim N(a)da(J_{lc}/J_c)^2/P(a)$ , where  $N(a)da$  is the number of stars in the interval  $(a, a + da)$ .

Close to the MBH,  $\Delta J_p \ll J_{lc}$ , so that any star in the loss-cone is immediately swallowed by the MBH. Since the time-scale for a change in angular momentum of order  $J_c$  is the relaxation time  $t_r$ , the rate at which stars are captured by the MBH in this “empty loss-cone” regime is

$$\Gamma(a)da = \frac{N(a)}{\ln(J_c/J_{lc})t_r(a)}da. \quad (2)$$

The logarithmic factor in the denominator stems from a modification of the DF due to the presence of the loss-cone [31]. Since inspiral occurs over many orbits, it is the empty loss-cone regime which is relevant for the GW event rate.

## Inspiral sources

Equation (2) assumes that a star that is captured at peri-apse is taken out of the system immediately. Such events indeed occur (for example when a CR has a wide orbit with peri-apse smaller than the Schwarzschild radius), but such stars do not contribute to the LISA detection rate<sup>1</sup>. In order to be detected by *LISA*, a star may start at a wide orbit, but must then spiral in until its period becomes comparable to  $P < 10^4$  s.

A star that starts spiraling in when its semi-major axis is very large, is unlikely to reach the MBH without plunging in, because it has to make a very large number of orbits. Since during these orbits its angular momentum changes randomly due to weak encounters with other stars, the probability is large that it will at some point be scattered into the MBH. On the other hand, a star that has initially a small semi-major axis, is likely to spiral in without being scattered into the loss-cone, since it loses energy quickly and has little chance to scatter significantly. Thus, there exists some critical semi-major axis  $a_{\text{GW}}$  that separates these two regimes. This critical value can be estimated as follows [21]:

The change in  $J$  of a star per orbital period  $P$  is  $\Delta J_p = (P/t_r)^{1/2} J_c$ . The time-scale for a change of order  $J$  is  $t_J = (J/J_c)^2 t_r$ . In particular, the time-scale for a change in  $J$  by the order of the loss-cone, is  $t_{lc} = (J_{\text{LSO}}/J_c)^2 t_r$ . Inspirals due to dissipation by GW emission happens on a time-scale  $t_0(a, J)$ , which for highly eccentric orbits has a very strong angular momentum dependence,  $t_0(J) \propto J^7$ . If  $t_{lc} \ll t_0(a, J \rightarrow J_{\text{LSO}})$ , the angular momentum will be modified even if the star has  $J = J_{\text{LSO}}$ . As a result it is very likely that the star will be scattered into the loss-cone (or away from it, to an orbit where energy dissipation is very weak). The approximate condition  $t_0(a, J \rightarrow J_{\text{LSO}}) < t_{lc}(a)$  translates into a maximal semi-major axis  $a_{\text{GW}}$  a CR must have in order to spiral in without plunging into the MBH, and become a *LISA* source. For MBHs,  $a_{\text{GW}} = \text{few} \times 0.01$  pc [21, 22, 23].

In order to test these ideas further, Hopman & Alexander [21] performed Monte Carlo (MC) simulations. In these simulations, stars started at some given energy and angular momentum, and at every time-step  $\delta t$ , the angular momentum changed randomly by an amount  $\delta J = (\delta t/t_r)^{1/2} J_c$ , and the energy was increased deterministically due to GWs by an amount  $\delta E = \dot{E}_{\text{GW}} \delta t$ . For each energy, the experiment was performed many times with different random numbers, and for each star it was denoted whether it entered the *LISA* band, or whether it was swallowed prematurely by the MBH because the angular momentum became smaller than that of the last stable orbit. The orbital quantities in these simulations were treated in a pseudo general relativistic form. If  $N_p(a)$  is the

---

<sup>1</sup> Our own Galactic center may be close enough to observe bursts of GWs when stars come close to the MBH at one single passage [40]. In the following I do not consider such events, which are not observable in extra-galactic nuclei.

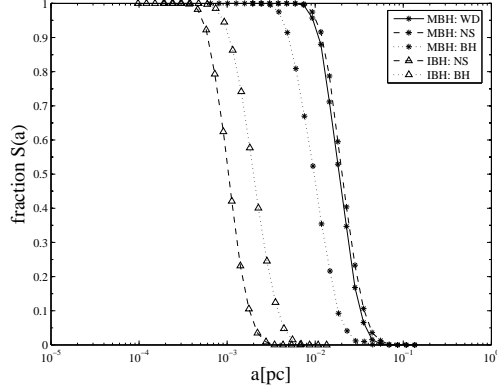


**FIGURE 1.** Dependence of the normalized fraction of inspiral events on initial semi-major axis, for the case of a MBH of  $M_{\bullet} = 3 \times 10^6 M_{\odot}$  (asterisks) and an IMBH of  $M_{\bullet} = 1 \times 10^3 M_{\odot}$  (triangles). The solid line is for WDs, the dashed lines for NSs, and the dotted lines for stellar BHs. Reprinted with permission from the *Astrophysical Journal*.

number of stars with some given initial  $a$  that are promptly swallowed, and  $N_i(a)$  the number of stars which spiral in slowly and become sources that can be observed with *LISA*, then the probability for inspiral is given by

$$S(a) \equiv \frac{N_i(a)}{N_p(a) + N_i(a)}. \quad (3)$$

In figure (1) the resulting function  $S(a)$  from the simulations performed by [21] is shown. The left two curves are the results for IMBHs and the three right curves for a MBH of mass  $M_{\bullet} = 3 \times 10^6 M_{\odot}$ . The function  $S(a)$  is equal to 1 for small  $a < a_{\text{GW}}$ , and drops very quickly to  $S(a) = 0$  for  $a > a_{\text{GW}}$ , in accordance with the qualitative picture given above. To account for the fact that not all stars that are captured become eventually observable by *LISA*, the inspiral rate is obtained by integrating equation (2) with  $S(a)$ ,

$$\Gamma = \int_0^{\infty} da S(a) \frac{N(a)}{\ln(J_c/J_{lc}) t_r(a)}. \quad (4)$$

The shape of  $S(a)$  was verified by  $N$ -body simulations [7] for tidal inspiral of MS stars near an IMBH, a process that is dynamically similar to GW dissipation [4, 25, 24].

For successful inspirals in the MC simulations by [21], the eccentricities were recorded at the point where the period was  $P = 10^4$  s. The DF of eccentricities was seen to be skewed towards high eccentricities (Fig. 2). Interestingly, this is in contrast with what is predicted for EMRIs that result from *indirect* capture of stars (see below).

## DYNAMICS WITHIN THE INNER FEW 0.01 pc

The EMRI event rate is determined by the dynamics and stellar content within  $a_{\text{GW}} = \text{few} \times 0.01$  pc, which determine  $N(a)$  and  $t_r(a)$  in Eq. (4). In this section, two important dynamical phenomena are discussed.

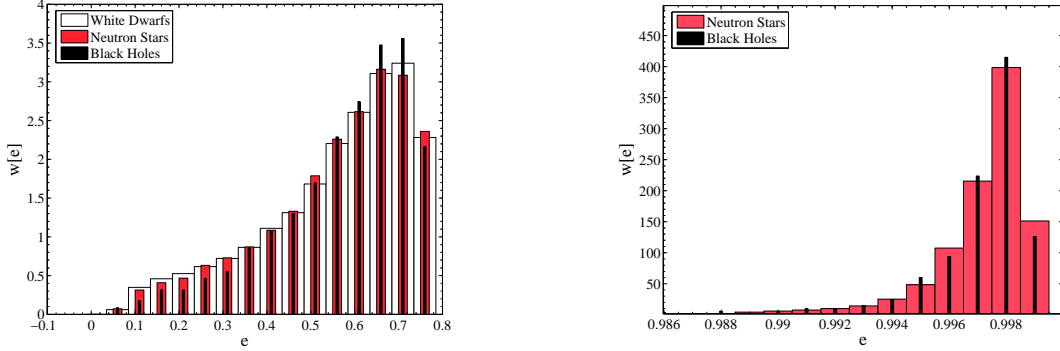


**FIGURE 2.** Eccentricity DF for orbits of  $P = 10^4$  s, from the MC simulations by [21]. The left figure is for MBHs with  $M_{\bullet} = 3 \times 10^6 M_{\odot}$ , and the right figure for IMBHs with mass  $M_{\bullet} = 1 \times 10^3 M_{\odot}$ . The eccentricities for IMBHs are so high, that the frequency may be too high to be observed by *LISA*. Reprinted with permission from the *Astrophysical Journal*.

## Mass segregation

When two stars of different masses interact gravitationally, there will be a tendency to divide their kinetic energy equally. While equipartition is never reached for a star cluster, this effect causes the massive stars to sink more effectively to the center than the lighter stars, and is known as mass segregation. Mass segregation near a MBH was first studied by [6] in the context of an old stellar population near an IMBH. They found that different species are distributed according to approximate power-laws with different slopes (see Eq. 1), and that the most massive particles have the steepest slopes and are thus more centrally concentrated. This effect was confirmed by  $N$ -body simulations by [8, 13], whose results were generally in good agreement with the [6] predictions. Simulations of mass segregation near MBHs were recently performed by [13] and [23]. Freitag et al. [13] performed extensive MC simulations [14] with different mass functions that included much larger mass ratios for the different stellar populations than were considered by [6]. Their simulations confirm the results by [6] that the massive species are steeper distributed than the lighter stars, although they find that the cusp of the lightest stars is even shallower ( $\alpha = 1.3$ ), and the more massive stars is steeper ( $\alpha \sim 2$ ) than those found by [6].

Hopman & Alexander [23] directly solved the multi-mass Fokker-Planck equations given by [6] for four species: MSs, WDs, NSs and stellar BHs. The equations are one dimensional and consider only the dynamics in energy space, but they added a sink term to calculate the rate at which stars reach the loss-cone in  $J$ -space. Like [13], they find that the steepest DF is that of the stellar BHs, with a slope of  $\alpha = 2$ . Within a distance of  $< 0.1$  pc of the MBH stellar BHs become the dominant CR in terms of numbers. Since the stellar BHs are more massive than the other stars, this also implies that the relaxation time decreases when compared to a single mass population; [23] find that close to the MBH it becomes as short as  $\sim 10^8$  yr. Using the relaxation time resulting from the steady state DF of the stars, they determined the probability function for successful inspiral, Eq. (3), with the MC method described in [21]. Finally, now that both the radial DF of stars and the inspiral probability function are known, the cumulative event rate can be

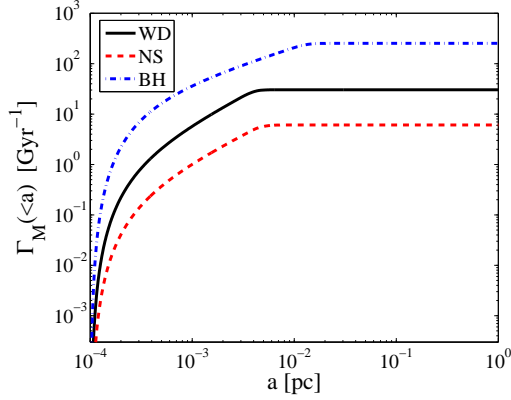


**FIGURE 3.** Cumulative rate of EMRI formation for stellar BHs (blue dashed-dotted line), WDs (black solid line), and NSs (red dashed line) as a function of the distance from the MBH. In spite of the fact that far away from the MBH WDs were assumed to be more abundant than stellar BHs by two orders of magnitude, stellar BHs dominate the even rate. Reprinted with permission from the *Astrophysical Journal*.

estimated for the different species with Eq. (4); the result for WDs, NSs and stellar BHs are given in Fig. (3). The total rate is clearly dominated by stellar BHs, and estimated to be of order  $\Gamma = \text{few} \times 10^2 \text{ Gyr}^{-1}$  per MBH system. Since stellar BHs also give a stronger signal due to their higher mass, it appears a robust result that the EMRI detection rate by *LISA* will be dominated by stellar BHs.

The DF of stars within the radius of influence depends not only on stellar dynamics, but also on poorly constraint quantities such as the star formation history and initial mass function outside the radius of influence  $r_h$  [10]. Even in our own Galactic center, there is no knowledge of the stellar content within  $a_{\text{GW}}$  [34]. EMRI observations by *LISA* may therefore provide a unique observation to the stellar populations very close to MBHs.

## Resonant relaxation

Near MBHs orbits of stars hardly precess if the enclosed mass in stars is small, and precession due to general relativistic effects can be neglected. It was shown [39, 38] that the resulting torques for such orbits lead to a relaxation mechanism that is much more efficient than two-body relaxation. This mechanism, known as *resonant relaxation* (RR), affects only the angular momenta of the stars, and not their energies.

If general relativistic effects are neglected, the RR time  $T_{\text{RR}}$  is given by

$$T_{\text{RR}} = A_{\text{RR}} \frac{M_{\bullet}}{M_{\star}} P(a); \quad (5)$$

here  $A_{\text{RR}}$  is a numerical factor which was estimated by [39] to equal  $A_{\text{RR}} = 3.56$ . Since  $T_{\text{RR}} \propto P(a)$ , the RR time decreases rapidly towards the MBH.

RR leads to a small enhancement of the tidal disruption rate, which is dominated by effects close to the radius of influence ( $r_h \sim 1$  pc), where  $T_{\text{RR}}$  approximately equals the non-resonant relaxation time. However, at the critical distance  $a_{\text{GW}} \sim 0.01$  pc, RR is

very efficient. As a result, the flow of stars towards the loss-cone is much more rapid than would be the case if relaxation were non-resonant, as is usually assumed. Hopman & Alexander [22] showed that the EMRI event rate is in fact dominated by RR, which increases the rate by nearly an order of magnitude.

The factor  $A_{RR}$  is not very well determined. If it is slightly larger than estimated by [39], the GW event rate will increase further. However, if  $A_{RR}$  is larger by an order of magnitude than estimated by [39], the loss-rate can be so large, that energy relaxation cannot replace the stars, which can in principle lead to a strong depression of the event rate [22]. It is therefore of interest to obtain further understanding of the details of RR.

## **INDIRECT CAPTURE OF EMRIS**

In the scenarios described above, a CR on a loosely bound orbit becomes tighter bound because it loses energy to the GWs themselves. This happens on extremely eccentric orbits ( $1 - e \sim 10^{-4}$ ), and even after the orbital frequency exceeds  $10^4$  Hz, the orbit is still eccentric (Fig. 2). There are several alternatives in which the CR does not lose its energy to GWs, but to other channels. Here three such mechanisms are discussed. Interestingly, these all have in common that the resulting eccentricities become very low,  $1 - e \sim 1$ .

### **Stellar formation in accretion disks**

When dense gas is present near a MBH in the form of an accretion disk, as is the case for active galactic nuclei, it may become self-gravitating, and stars can form in the disk. Our own Galactic center provides evidence that this has happened there recently ( $< \text{few Myr}$ ), because there are disks of young OB stars present [30, 16], which are best explained by stellar formation in an accretion disk [30, 29, 35]. Levin [28] argued that massive stars formed in accretion disks may have enough time to evolve and become stellar BHs, and spiral in due to interaction with the gas in the disk within the life time of the accretion disk. The interaction with the gas flow is likely to keep the orbit close to circular, so this would lead to zero-eccentricity *LISA* EMRIs. The event rate depends clearly on a large number of uncertain factors, such as the efficiency of star formation in disks, the accretion rate of the stars in the disks, and the inspiral time within the disk. However, [28, 29] found that it is not implausible that the contribution to the total *LISA* event rate may be considerable.

### **Tidal binary disruption**

The majority of stars in galaxies reside in binaries. Near MBHs the binary fraction may be considerably lower than average, because of the high velocity dispersion: this implies that typically, when a single star encounters a binary, the binary star becomes less tight [18]. Nevertheless, it is plausible that near the radius of influence of a MBH there is a binary fraction of at least a few percent [37].

When a binary is scattered to a very eccentric orbit, it may be tidally disrupted by the MBH. In that case, one star is ejected at very high velocity, and the other star becomes tightly bound to the MBH [19, 42, 17, 37]. In this case it is the ejected star that 'absorbs' the orbital energy; such hypervelocity stars have now been observed in our Galaxy [9].

If the star that remains bound to the MBH is a CR, it can spiral in due to GW emission. Miller et al. [32] found that this results in zero-eccentricity *LISA* orbits, and that the event rate may well exceed the event rate of direct inspirals, although uncertainties are considerable, in particular due to the unknown fraction of binaries near MBHs, and the frequencies in which CRs are present in such binaries.

### **Remnants of ultraluminous X-ray sources**

It was argued by [21] that for direct capture of a CR by an IMBH, the resulting orbits will be so eccentric that even if a star is captured, it will not be 'visible' by *LISA* because the frequency will be too high. However, this does not necessarily imply that IMBHs will not be observable at all by *LISA*. A possibility that was considered by [24] is that a main sequence star that is *tidally* captured by an IMBH will evolve later to a stellar BH and spiral in due to GW emission. Since the tidal forces have circularized the orbit, this will lead to a low eccentricity and low frequency orbit that can be observed by *LISA*. Before the super nova explosion, the star may fill its Roche lobe and be observable as an ultraluminous X-ray source [25]. Observational support for this scenario comes from the ultraluminous X-ray source in M82, which is perhaps the best IMBH candidate. This source has a 62 day period in its X-ray luminosity, which has been interpreted as an orbital period, and is best explained if the accretor is an IMBH [27, 36].

As for the previous scenarios, it is highly uncertain how many of these sources will be observable by *LISA* (if any). [24] estimated from the observed ultraluminous X-ray populations that there is a good probability to observe several IMBH-CR binaries with *LISA*.

### **CONCLUSIONS**

I have discussed the formation of EMRI sources that will be observable by *LISA*. The event rate for directly captured EMRIs is of the order of  $\text{few} \times 10^2 \text{Gyr}^{-1}$  per MBH, with stellar BHs the dominant species. This event rate will lead to many observable sources for *LISA* [10]. EMRIs formed by direct capture are typically highly eccentric. Alternative mechanisms for EMRI formation lead to very low eccentricities, so that the resulting eccentricity DF will probably be bimodal.

### **ACKNOWLEDGMENTS**

I thank the organizers of the LISA6 conference for a very stimulating meeting.

## REFERENCES

1. Alexander, T. 1999, *ApJ*, 527, 835
2. —. 2005, *Phys. Rep.*, 419, 65
3. Alexander, T., & Hopman, C. 2003, *ApJL*, 590, L29
4. Alexander, T., & Morris, M. 2003, *ApJL*, 590, L25
5. Bahcall, J. N., & Wolf, R. A. 1976, *ApJ*, 209, 214
6. —. 1977, *ApJ*, 216, 883
7. Baumgardt, H., Hopman, C., Portegies Zwart, S., & Makino, J. 2005, *ArXiv Astrophysics e-prints*, astro-ph/0511752
8. Baumgardt, H., Makino, J., & Ebisuzaki, T. 2004, *ApJ*, 613, 1143
9. Brown, W. R., Geller, M. J., Kenyon, S. J., & Kurtz, M. J. 2005, *ApJL*, 622, L33
10. de Freitas Pacheco, J. A., Filloux, C., & Regimbau, T. 2006, *ArXiv Astrophysics e-prints*, astro-ph/0606427
11. Freitag, M. 2001, *Classical and Quantum Gravity*, 18, 4033
12. —. 2003, *ApJL*, 583, L21
13. Freitag, M., Amaro-Seoane, P., & Kalogera, V. 2006, *ArXiv Astrophysics e-prints*, astro-ph/0603280
14. Freitag, M., & Benz, W. 2002, *A.A.P.*, 394, 345
15. Gair, J. R., Barack, L., Creighton, T., Cutler, C., Larson, S. L., Phinney, E. S., & Vallisneri, M. 2004, *Classical and Quantum Gravity*, 21, 1595
16. Genzel, R., et al. 2003, *ApJ*, 594, 812
17. Gualandris, A., Portegies Zwart, S., & Sipior, M. S. 2005, *MNRAS*, 363, 223
18. Heggie, D. C. 1975, *MNRAS*, 173, 729
19. Hills, J. G. 1988, *Nature*, 331, 687
20. Hils, D., & Bender, P. L. 1995, *ApJL*, 445, L7
21. Hopman, C., & Alexander, T. 2005, *ApJ*, 629, 362
22. —. 2006, *ArXiv Astrophysics e-prints*, astro-ph/0601161 (accepted to *ApJ*)
23. —. 2006, *ArXiv Astrophysics e-prints*, astro-ph/0603324 (accepted to *ApJL*)
24. Hopman, C., & Portegies Zwart, S. 2005, *MNRAS*, 363, L56
25. Hopman, C., Portegies Zwart, S. F., & Alexander, T. 2004, *ApJL*, 604, L101
26. Ivanov, P. B. 2002, *MNRAS*, 336, 373
27. Kaaret, P., Simet, M. G., & Lang, C. C. 2006, *Science*, 311, 491
28. Levin, Y. 2003, *arXiv*, available at <http://xxx.lanl.gov/abs/astro-ph/0307084>
29. —. 2006, *ArXiv Astrophysics e-prints*, astro-ph/0603583
30. Levin, Y., & Beloborodov, A. M. 2003, *ApJL*, 590, L33
31. Lightman, A. P., & Shapiro, S. L. 1977, *ApJ*, 211, 244
32. Miller, M. C., Freitag, M., Hamilton, D. P., & Lauburg, V. M. 2005, *ApJL*, 631, L117
33. Miralda-Escudé, J., & Gould, A. 2000, *ApJ*, 545, 847
34. Mouawad, N., Eckart, A., Pfalzner, S., Schödel, R., Moulataka, J., & Spurzem, R. 2005, *Astronomische Nachrichten*, 326, 83
35. Nayakshin, S., & Sunyaev, R. 2005, *MNRAS*, L94+
36. Patruno, A., Portegies Zwart, S., Dewi, J., & Hopman, C. 2006, *MNRAS*, L49+
37. Perets, H. B., Hopman, C., & Alexander, T. 2006, *ArXiv Astrophysics e-prints*, astro-ph/0606443
38. Rauch, K. P., & Ingalls, B. 1998, *MNRAS*, 299, 1231
39. Rauch, K. P., & Tremaine, S. 1996, *New Astronomy*, 1, 149
40. Rubbo, L. J., Holley-Bockelmann, K., & Finn, L. S. 2006, *ArXiv Astrophysics e-prints*, astro-ph/0602445
41. Sigurdsson, S., & Rees, M. J. 1997, *MNRAS*, 284, 318
42. Yu, Q., & Tremaine, S. 2003, *ApJ*, 599, 1129